Characterisation of Scintillation effect on Galileo Sensor Station Continuity of Service

Stéphane Lannelongue, Thales Alenia Space France
Hervé Guichon, *Thales Avionics*
Yannick Beniguel, *IEEA*
Massimo Crisci, Francisco Amarillo, *European Space Agency.*

BIOGRAPHY

Stéphane LANNELONGUE is a Senior engineer in the navigation system engineering department of THALES ALENIA Space France. He received in 1996 a M. Sc. engineer degree in electronics and signal processing from ENSIEG, France. Since 1997 he has been working in the field of satellite navigation successively in CNES, European Space Agency, and THALES ALENIA SPACE. Among other, he was technically responsible of the EGNOS integrity algorithm development and was deeply involved in the elaboration of the Galileo integrity concept. Since 2005, he is leading the performance allocation management activity of the Galileo Mission Segment.

Hervé GUICHON has a Master's degree in Aeronautical Engineering (ENSAE - Toulouse, France 1975). He was involved in several programs of Magnetic Anomaly Detection (airborne and buoys, in cooperation with Magnavox from 1988 to 1993). Since 1994 he has been developing GPS/GLONASS receivers, with focus on signal processing; he is now GNSS Systems Engineer and design authority of the Ground Receiver Chain for the Galileo project.

Yannick BENIGUEL has a Ph.D. from Paris VI University. He is the head of IEEA Company, working mainly on antennas and propagation topics. He has been involved in several earth space propagation projects for navigation purposes, with ESA / ESTEC. He has developed under an ESTEC contract the Global Ionospheric Propagation Model (GISM).

Dr. Massimo CRISCI has a Ph.D. in Automatics and a Master's degree in Electronics Engineering. He is working as Radio Navigation and Signal Processing Engineer for ESA (TEC/ETN), part of the GALILEO/GIOVE System/GMS engineering team, where he is currently in charge of GRC and SIV tool procurements, and of the GALILEO/GIOVE SIS Verification and Validation activities.

Francisco AMARILLO-FERNANDEZ…

INTRODUCTION

European Commission in cooperation with the European Space Agency is currently developing a Global space based Navigation system name Galileo. This system is the European counterpart of the Navstar GPS American system. It is composed of 27 satellites in a medium orbit (≈23000 km altitude) completed with three spares. Galileo system is specified in order to provide an integrity service with high availability and continuity performance. Such level of performance is furthermore required to be met in severe interference and ionosphere environment conditions. The Galileo integrity service being provided on a dual frequency basis, the level of performance is not that much disturbed by the variation of the TEC (Total electron Content). However the provision of a reliable integrity service relies on the availability and quality of the data collected by the network of sensor station used to monitor the satellite signal in space. Main common effects of scintillation are fading in terms of signal power and rapid phase variations susceptible to induce cycle slips or loss of lock at receiver level.

It is therefore critical that the Galileo system, and in particular the receiver deployed within the sensor stations, provide a certain level of robustness against such phenomena. Note that such effect is emphasized by the fact that the Galileo network is deployed worldwide in order to provide a full coverage, including the equatorial and polar regions particularly subject to severe scintillation conditions.

This paper focuses on the analysis of scintillation impact on receiver tracking performance. Starting with stringent and conflicting requirements, this study has led to the definition of acceptable operating points at receiver level.

The main topics covered in this activity are:

- Characterising of the statistical and dynamic behaviour of scintillation phenomena based on time series produced by the GISM model.
- Qualitative receiver behaviour in strong scintillation conditions, showing critical issues and trade-off.
- Elaboration of an optimal functioning point at receiver level with respect to robustness to scintillation based on trials performed with the GISM time series.
- Review of the available model in literature in order to predict receiver performance with respect to loss of lock performance with respect to S4 and Sigma phi parameters. This covers the comparison of the basic assumptions considered in order to adapt those models together with receiver optimised tuning.

- Proposition of models refinement in order in order to be able to extrapolate receiver performance among a wide range of scintillation conditions.

GALILEO CONTEXT

The main differentiator of Galileo system with respect to GPS is the capability to provide real time integrity information to the user. This consists in monitoring in real time the accuracy of the orbit and clock synchronization core product broadcast through the satellite signal in space and send within the required time to alarm (6 seconds) warning to users in case of satellite failure. Current GPS system does not provide this service in stand alone and need to be augmented with SBAS system (Space Based Augmentation System) such as WAAS in the USA and EGNOS in Europe.

The provision of real time integrity data requires an accurate monitoring of the satellite considering the two following constraints:

- The service to be provided by Galileo is tailored for civil aviation applications. It needs then: to be available quasi 100% of the time.
- The monitoring needs to be continuous in the sense that when the service is available at T0, it shall remain available until T0 plus 15 seconds in order to enable the completion of critical phase of flight.

Galileo service is to be provided worldwide. This means that the satellite shall be monitored all the time, whatever their location. This implies to deploy a worldwide monitoring station network. The following figure depicts the approximate location of the Galileo Sensor Stations (GSS) currently network planned to be deployed in order to be able to monitor in real time the Galileo satellites with the required accuracy.

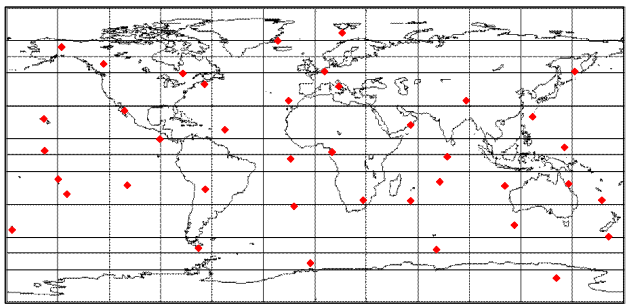

Figure 1: Definition of geo-magnetic equatorial area

In order to first design the monitoring station network enabling to fulfil Galileo mission requirement, and second to quantify the performance of the system it is mandatory to consider all the potential sources of system unavailability. One of the main sources of data unavailability that has been identified is the phenomena of ionosphere scintillation. Indeed Scintillation causes radio frequency signal amplitude fades and phase variations as satellite signals pass through the ionosphere. Such effect may induce loss of lock or cycle slips on ranging signals broadcast by Galileo satellites making them totally useless for accurate integrity information determination. Scintillation occurs mostly during the peak of solar cycle. It may be severe in equatorial regions in between +/- 20 degrees (geomagnetic equator) after sunset, and to a certain extend polar and auroral regions. Scintillation has typically a minimum impact in mid-latitude regions.

Finally, the Galileo system is designed in order to be operational for several tens of years. It shall therefore be robust to the different environment conditions that may be encountered during this period especially regarding scintillation. The following picture details the mean monthly sun spot representative of the solar activity recorded during the latest 50 years

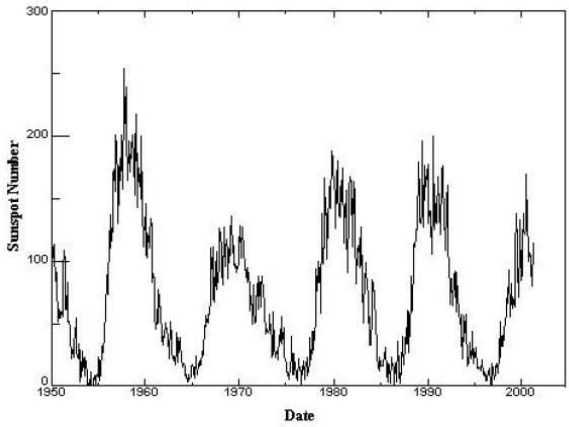

Figure 2: Sun Spot Numbers from 1950 to 2000

The problem is to determine the overall system performance: accuracy of orbitography, availability of integrity, which depend on the statistical distribution over space and time of the accuracy and availability of measurements from all Galileo Sensor Stations

SCINTILLATION CHARACTERISTICS

Ionosphere scintillation is a well-known phenomenon affecting radio wave propagation through ionosphere. It was first studied in the context of radio-sounding experiments, and received a lot of attention since the development of GPS, and in particular in the course of the WAAS and EGNOS programs and their planned extension to equatorial areas.

It is not the purpose of this paper to analyse in detail the physical aspects of ionosphere scintillation. A good introduction and comprehensive list of references can be found in [01] and [02]. A brief reminder of main characteristics of ionosphere scintillation is provided below.

Ionosphere scintillations are produced by changes in the phase velocity of a satellite signal wave front as it passes through plasma-density irregularities in the ionosphere. As the wave propagates towards the ground, mutual interference creates complex amplitude and phase diffraction patterns. Scintillations are produced when these spatial diffraction patterns are transformed into temporal ones, either through relative motion between the

receiver and the patterns, or by changes in the structure of the irregularities with time.

Scintillations occur predominantly in the equatorial band that extends from about 20°S to 20°N of the magnetic equator, and in the auroral and polar cap regions. The processes that produce scintillations in these two regions are quite different, leading to significant differences in the characteristics of the resulting scintillations.

Auroral and polar cap scintillations are mainly the result of geomagnetic storms. Unlike equatorial scintillations, they show little diurnal variation in their rate of occurrence, and can last from a few hours to many days, beginning at any time during the day.

Equatorial scintillations, on the other hand, are produced by irregularities in the F-layer of the equatorial ionosphere following the passage of the evening gradient and tend to disappear soon after midnight. Equatorial scintillations tend to be worse during the years of solar maximum when the anomaly is at its greatest; they also show a strong seasonal dependence.

For analysis of receiver behaviour, the parameters used to characterize scintillation are usually :

- the RMS phase σϕ

The phase scintillation is considered to follow a zero-mean normal Probability Density Function. Its Power Spectrum Density can be approximated by :

$$S_\varphi(f) = \frac{T}{\left(f^2 + f_0^2\right)^{p/2}} \quad \text{rd2/Hz} \qquad \text{Eq. (1)}$$

where T is the spectral strength, f0 is a frequency corresponding to the maximum irregularity size, and p is the spectral index (typically 2.5 at equatorial latitudes).

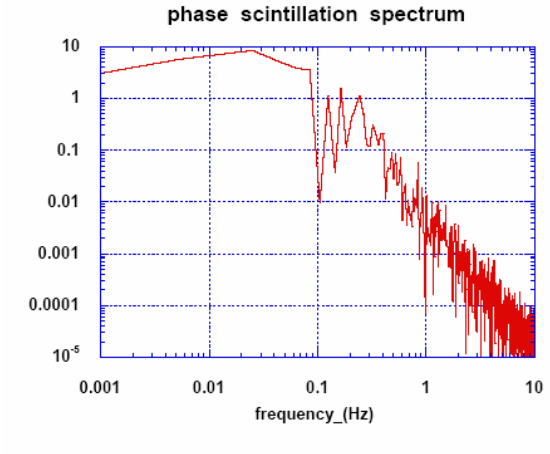

Figure 3: Phase Error Power spectrum Density

- the normalized RMS intensity

$$S_4 = \left(\frac{\langle I^2 \rangle - \langle I \rangle^2}{\langle I \rangle^2} \right)^{1/2} \qquad \textbf{Eq. (2)}$$

where $I=A^2$ is the signal intensity.

The amplitude A follows the Nakagami distribution :

$$p(A) = \frac{2.m^m.A^{2m-1}}{\Gamma(m)}.\exp\left(-m.A^2\right) \quad \textbf{Eq.(3)}$$

where Γ( ) is the Gamma function and $m = S4^{-2}$

The PSD of the amplitude follows a law similar to (1), with a spectral index decreasing from 3 to 2 with increasing S4 values.

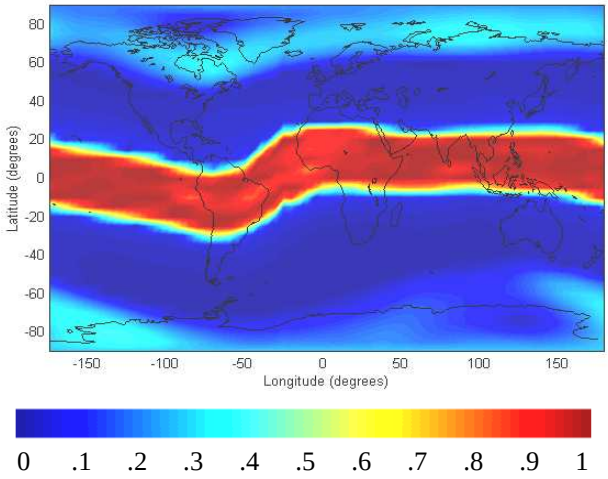

Figure 4 Scintillation Index Map

For the Galileo program, a set of scintillation conditions has been proposed by ESA [03]. The reference ionospheric model to be used for the program is GISM [04], which was developed previously by IEEA under ESA contract. The NeQuick model is used to generate the electron-density content, and a so-called "multiple phase-screen" model to compute the time and space distribution of the characteristic parameters S4 and σϕ. The following figure shows the geographical distribution of the maximum S4 parameter observed over one day. It underlines the dependency with the magnetic equator.

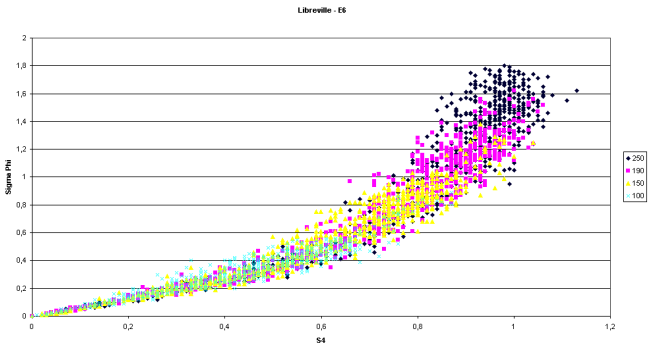

Figure 5 Scintillation Index Statistics

IMPACT ON GALILEO SENSOR STATIONS

The following figure computed with the Nakagami function shows the cumulative probability to have power fading larger than a certain number of dB. For S_4 equal 1, it can be seen that fading in between 10 and 20 dB are not remote. The probability to have a fading of 10 dB or more is 10% whereas the probability to have a fading of 20 dB or more is equal to 1%. For smaller S_4 equal to 0,3

the probability to have strong fading gets much smaller. It represents less than 1E-8 for fading larger than 10 dB.

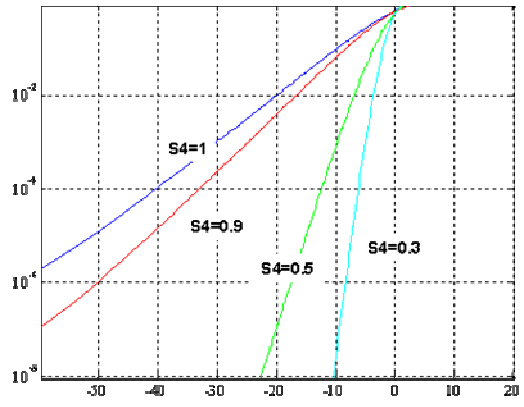

Figure 6 : Fading (dB) probability according to S_4

The following figure represents an output of the GISM with a S_4 parameter equal to 1. This shows that the probability to have strong fading larger than 20 dB is indeed not negligible and occurs a few times over 50 seconds.

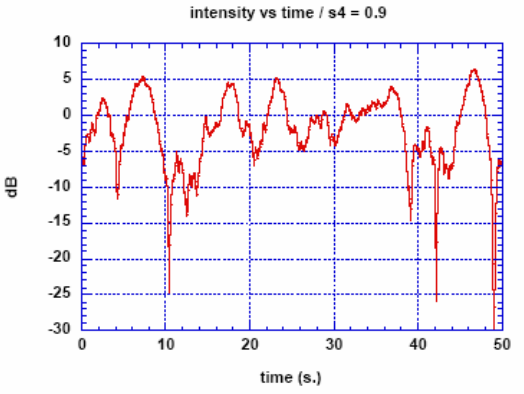

Figure 7: Power Fading (dB) time series

The following figure shows some statistics on the duration of the fading that is a key parameter in order to determine the receiver response to scintillation phenomena. For a S_4 equal to 0.9, fading of –15 db does not last more than 0.1 second.

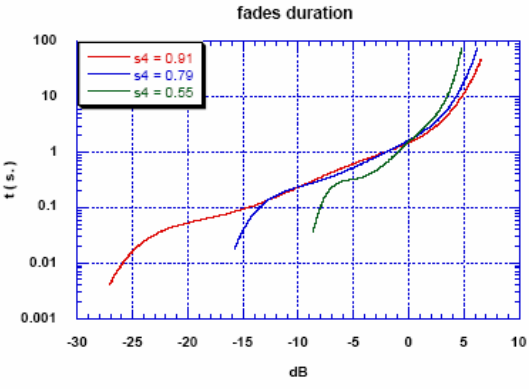

Figure 8 : Fades duration versus depth

Phase variations have the two following characteristics:

- It follows a zero mean gaussian distribution
- The 1-sigma value in radian is equal to σ_Φ.

Typically the σ_Φ parameter is about the same order of magnitude as the S_4. Its value varies in between 0 and 2 as showed in Figure 4. It is commonly agreed that the phase error budget that can be allocated to scintillation is the high frequency error above 0.1 Hz. The low frequency variations are assumed to be TEC variations following $1/f^2$ model. The following figure details the typical spectrum of the scintillation phase error.

An important point to characterize driving the capability of the Galileo ground receiver to cope with scintillation is the dynamic on the phenomena. The following figures show the correlation function of amplitude and phase scintillation phenomena for S_4=0.9. It demonstrates that the correlation of the phenomena is less than 1 second.

Such analysis is important mainly for two aspects:

1- Receiver response to fading is highly driven not so much by the depth of the fading but by its duration. If the correlation time of the phenomena is small, the fading events are likely to be more numerous but their duration will be smaller. If the fading duration is smaller than the receiver bandwidth, the receiver should be able to support it with very limited performance degradation.

2- To assess the impact of scintillation on the GMS continuity performance. Indeed such requirements are derived from civil aviation requirements and hence, expressed over 15 seconds. Therefore it requires to identify the number of independent samples within this exposure time. Based on the following plot it can be estimated that the time between independent samples is much smaller than 15 seconds, therefore the number of independent samples during 15 seconds is selected equal to 15.

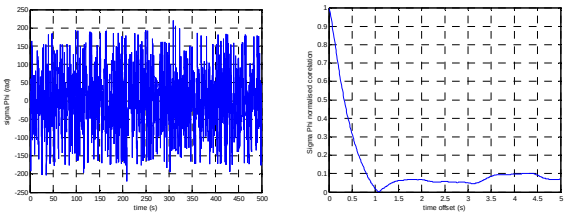

Figure 9: Phase Scintillation Correlation time

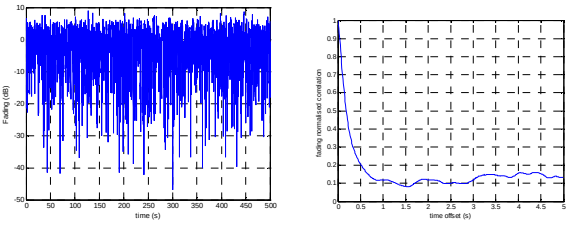

Figure 10: Amplitude Scintillation Correlation time

A key parameter to take into account at GMS level is that scintillation has a very specific time and geographical distribution.

1- It mainly affects stations that are localised on the geo magnetic equator (+/- 20 degrees) and to certain extend stations in polar areas. Station in mid latitude regions are almost not affected. Only lines of sight piercing the ionosphere at equatorial level may be affected. With the current GMS networks the number of stations located in the critical area is identified in the following table. On a 40 GSS stations network, 14 stations are within the geomagnetic equator, and therefore, potentially subject to severe scintillation
2- Stations in the equatorial regions are not affected all the time. The scintillation phenomenon lasts only a few hours after sunset. This means that at first order, only two to four stations may be affected at the same time.
3- When a station is affected, all the lines of sight are not impacted the same way.

In order to characterise the dispersion of scintillation phenomena, the GISM model was run simultaneously on the 50 stations over 56 hours from October 22nd, 2004 0h00 (sampling time 300 seconds). A solar flux of 300 was considered.

In order to characterise the scintillation phenomena at station level a first indicator was computed for each station. This is the number of occurrence of S_4>0.7 recorded on all line of sight and all time step over the simulation period.

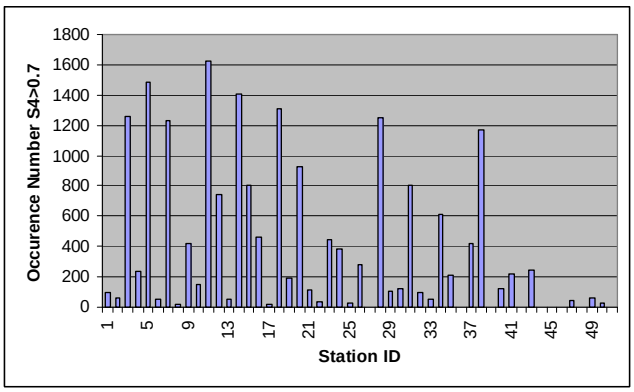

Figure 11: Geographic Distribution of S_4 (SF300)

It confirms that stations are very differently affected according to their location. The following figure shows the temporal distribution of the S_4 over two days according to the day hour. The scintillation affects the stations mainly during a few hours after sunset from 17h00 to 01h00.

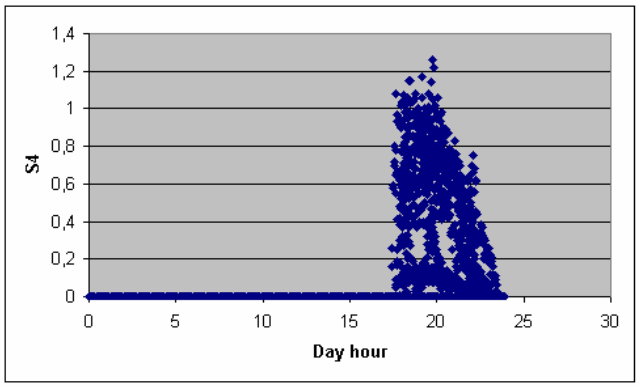

Figure 12: Temporal Distribution of S_4 (Djibouti)

When the location is affected all the satellites in sight are not affected the same way. The following diagram details the S_4 for all the satellites in sight of Djibouti station at 20h00. Satellites affected by a S_4 of 0 are actually not in sight of the station. Out of the 12 satellites in sight, 6 are affected by a S_4 larger than 0.5.

RECEIVER LOOP OPTIMISATION

In presence of scintillation, the tracking error of the receiver carrier loop consists of the thermal noise (linked to amplitude scintillation) and the dynamic response of the loop to input phase variation.

The error variance due to phase input decreases with increasing loop bandwidth (a wider loop tracks more easily a given input phase dynamics). Conversely, the thermal phase error decreases with loop bandwidth. This trade-off is well known and has for example been described in [02].

In the case of a static receiver like Galileo Receiver, the optimum loop BW will depend on the relative weight of phase and amplitude scintillation, as well as the quiescent C/N0.

The main concern for the GRC in specified conditions is the very deep amplitude fading occurring every several tens of seconds. Therefore one driving parameter for the receiver robustness is the prevailing signal-to-noise-ratio C/N0, which is itself mainly dependent on interference environment of the GSS stations.

The main goal of this study was to find an acceptable compromise between these two conflicting environments, aiming at satisfying at the same time the stringent requirements on cycle-slip and loss-of-tracking probabilities, including measurement accuracy, and accounting for receiver constraints, e.g. measurement de-correlation.

The loop simulation under scintillation allows to determine the bandwidth providing the best robustness trade-off between amplitude and phase scintillation. Without amplitude fading, it is of course easy to make the loop track most phase steps by increasing the loop BW:

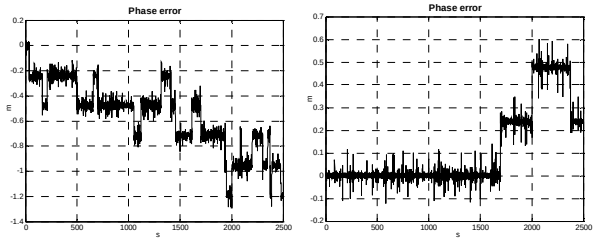

0.2 Hz 2 Hz

Figure 13 – Phase scintillation only

However, accounting for amplitude scintillation, this would be at the expense of a high loss-of-lock rate, or an unrealistically high C/N0 limitation :

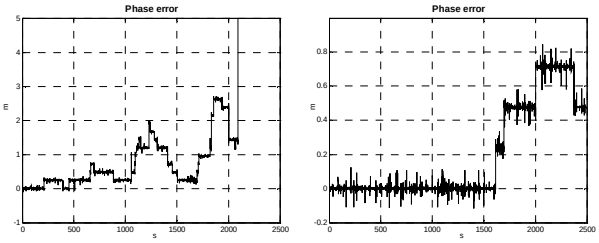

30 dBHz 60 dBHz

Figure 14 -Influence of amplitude scintillation (2Hz BW)

The final (relatively broad) compromise between scintillation, dynamic response and false lock leads to a noise BW around 1 Hz. Indeed, at S4 larger than 0.7 the time series obtained from the GIMS model exhibits some rapid variations larger than one cycle combined with strong fades. In those conditions, the strong fade blinds momentarily the PLL. When the fading disappears, although the phase has rotated of several cycles, the PLL locks again on the phase ambiguity that is in between +/- cycle compare to the value before fading. The dynamic of the variations make them not possible to follow even with a wide bandwidth. On the other hand a wide bandwidth would more sensitive to fading.

Furthermore, this loop satisfies the requirement of "non-correlation of measurements at 1s" that is necessary for an integrity monitoring network in order not to jeopardise the time to alarm performance of the total system.

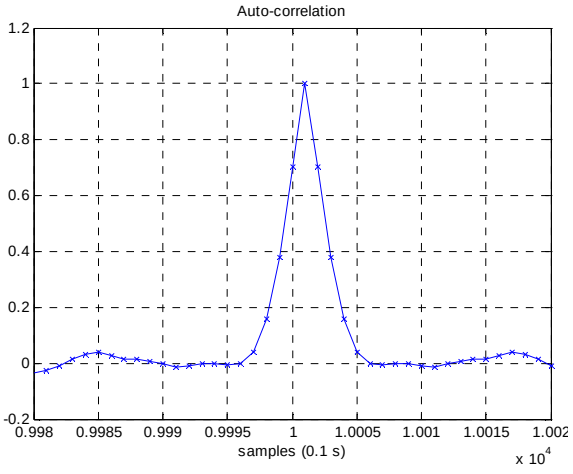

Figure 15 – Phase measurements autocorrelation

RECEIVER LOSS OF LOCK MODELS

The strategy in order to quantify the Loss of Lock probability is to compute for a certain C/N0 without scintillation the probability that the C/N including fading drops below the tracking threshold. Continuity requirements are applicable to dual-frequencies services that necessitate the combined use of code and phase measurements on the two frequencies. Therefore the receiver tracking threshold shall be estimated as the minimum C/N0 enabling to maintain lock on the code and phase on the both frequencies.

As detailed in [RD-11] the condition in order for a loop bandwidth not to loose lock is that the error remains within the linear part of the discriminator. For GPS signals, the fact to have a navigation message on the top of the pseudo random code forces to use a Costa Loop for phase tracking. For Galileo the fact to have a pilot signal free of navigation message enables to select a PLL with a 4-quadrants discriminator. This has the advantage to increase the linear part of the discriminator by a factor 2 that implies a 6 dB additional increase in terms of robustness compare to GPS C/A. A rule of thumb commonly used in order to define the tracking threshold is to define it as the minimum C/N0 necessary in order to maintain lock with a probability of 0.999. For a PLL, the phase discriminator can be considered as linear until 90 degrees. Therefore the receiver can maintain lock on the phase until the error remains below 30 degrees. .

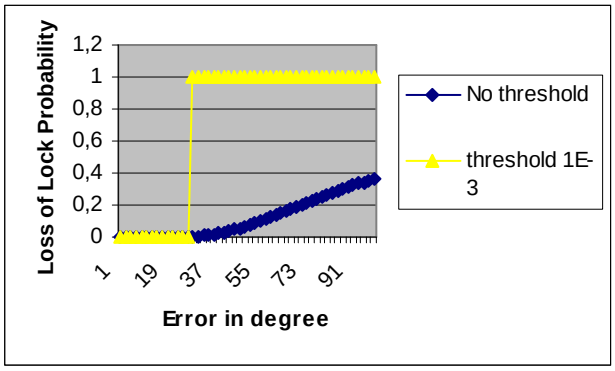

Figure 16: Loss of Lock probability according to phase error in degree.

The phase error can be approximated with the following formula ([RD-11]):

$$\sigma_{PLL} = \frac{360}{2\pi}\sqrt{\frac{B_n}{C/N_0}} \qquad \textit{Eq.(4)}$$

In theory the signal should be lost as soon as the available C/N (including fading) drops below the tracking threshold. Considering the Nakagami distribution, the figure 3 shows the occurrence probability of a fading according to its amplitude. This enables to compute the probability of loss of lock according to the C/N0 available without fading. The following tables show the obtained results with a tracking threshold equal to respectively 18 dB.Hz and 7 dB.Hz.

C/N0 (dB.Hz)	25	30	35
Fading (db)	*7*	*12*	*17*
S_4=1	2.0E-1	6E-2	2E-2
S_4=0.9	1.4E-1	3.6E-2	1E-2
S_4=0.5	9E-3	1.4E-4	1.6E-6
S_4=0.3	1.8E-5	2E-10	1E-15

Table 1 : Theoretical Loss Of Lock performance with 18 dB.Hz threshold

C/N0 (dB.Hz)	25	30	35
Fading (db)	*18*	*23*	*28*
S_4=1	1.6E-2	5.0E-3	1.6E-3
S_4=0.9	6.8E-3	1.6E-3	4.0E-4
S_4=0.5	6.2E-7	6.4E-9	6.3E-11
S_4=0.3	na	na	na

Table 2 : Theoretical Loss Of Lock performance with 7 dB.Hz threshold

However, such theoretical analysis has the strong limitation not to consider in any manner the duration of the fading. It assumes that the fading is constant over the whole integration time of the Loop (either PLL or DLL), which can be considered as an unrealistic assumption for Galileo ground receivers considering that the fadings are very short events (usually less than a few milliseconds or even microseconds). The probability to have strong fades larger than one second is very remote and cannot be taken into account in the present modelling.

The correlation between the fades duration, the loop bandwidth and the loss of lock probability is as follows:

- When the loop integration time is smaller than the fading duration, the global C/N0 is not improved after integration and therefore remains too low to maintain tracking.
- On the other hand if the integration time is larger than the fading duration, the PLL can take advantage of the part of the integration time during which the C/N is nominal (or quasi nominal) to coast though the strong fading and therefore maintaining lock.

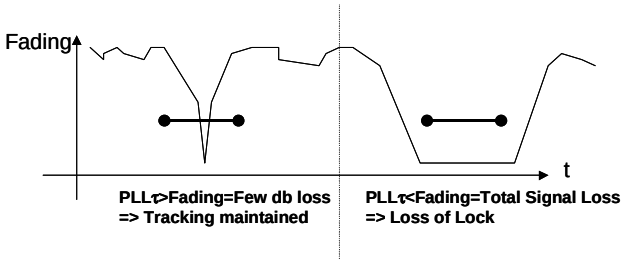

Figure 17: Qualitative description of PLL bandwidth impact on Receiver robustness to scintillation

The following figure represents the strongest fade observed on a fading time serie obtained with the GISM over a period of 500 seconds.

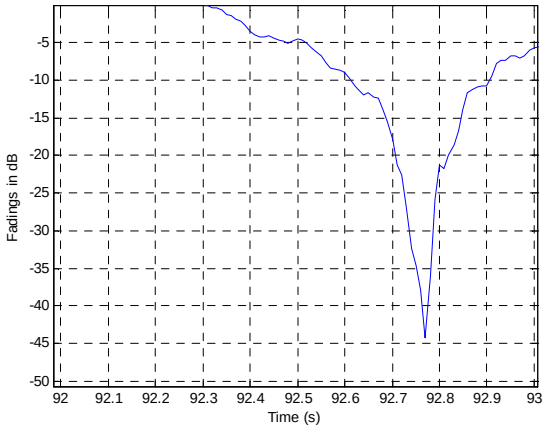

Figure 18: GISM Fading time series, general + zoom

It can be seen that the time during which the fade is larger then 20 dB lasts barely more than 100 ms. In case the C/N available crosses the tracking threshold it is very unlikely that it lasts more than a few milliseconds. The following picture details the equivalent C/N0 integrated in a 1-Hz loop bandwidth. What can be seen is that the fading are very short with respect to the loop integration time and that therefore a C/N0 of 35 dB.Hz would be reduced by only around 10 dB.

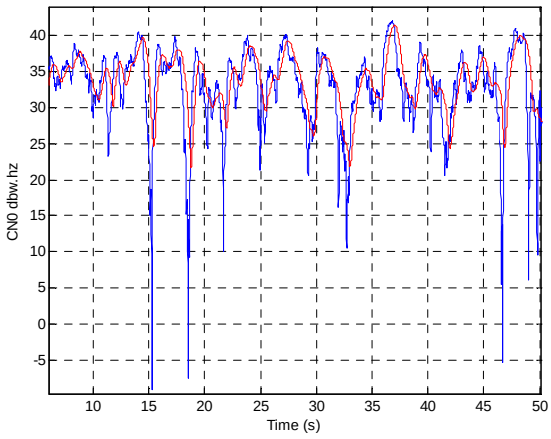

Figure 19 : CN0 Equivalent and PLL 1 Hz noise bandwidth (blue curve: without filtering, red curve: with filtering)

This confirms that the usual technique that can be found in literature in order to assess the loss of lock probability is not adequate for narrow loop bandwidth. For wide loop bandwidth (100 Hz), the integration time of the PLL is 10 ms. On such short time period, it makes more sense to consider that there is only a single independent sample on the integration time period and that the fading remains constant (although it is not exactly what comes out from the GISM model). Under these conditions standard formula are more representative.

The following figure on the left shows a zoom on the 16 more important fades observed on the time period of 500 seconds (worst fade centred on 0.5s). It highlights that, as expected, the fade is far to be constant over one second. The fade has time, from its nominal value, to get

down to the worst fade and come back to quasi-nominal situation. For some of the deep fades, two transitions can even be observed.

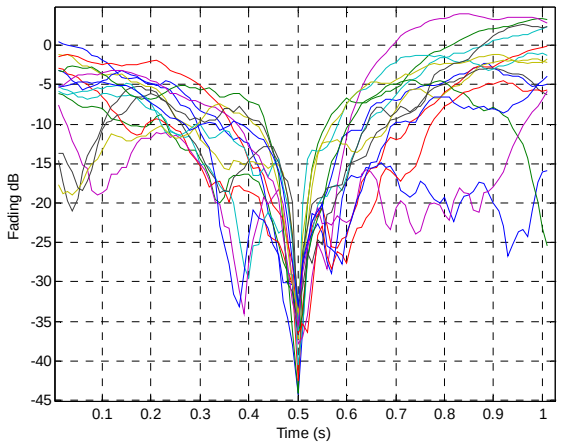

Figure 20: Fades temporal characterisation over 1 second

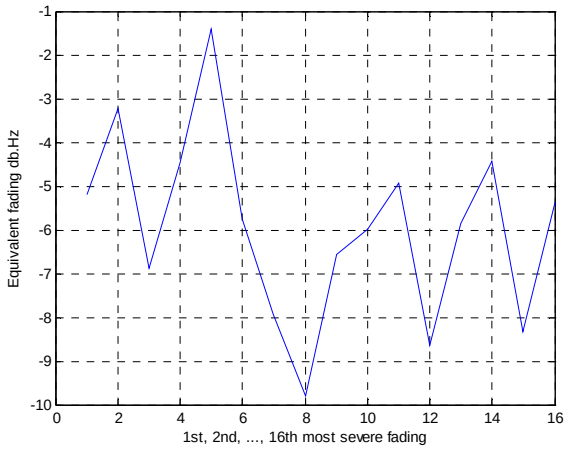

Figure 21: Fades temporal characterisation over 1 second

Figure 21 shows for each worst fades (starting from the worst one) the associated C/N0 degradation on the loop integration time. What is interesting to notice is that the worst C/N0 degradation is not observed for the worst fade. There is no direct correlation between the depth of the fade and the C/N0 degradation. Next figure focuses on the worst equivalent C/N0 degradation observed on the time series analysed. The equivalent C/N0 (red curve) drops down to 20 db.hz whereas the fading on the integration time remains below 37 db (instantaneous C/N0 equal to –2 dB.Hz). The worst instantaneous fade is observed in another part of the time serie at –45 dB and induces a C/N0 degradation of 5 dB only.

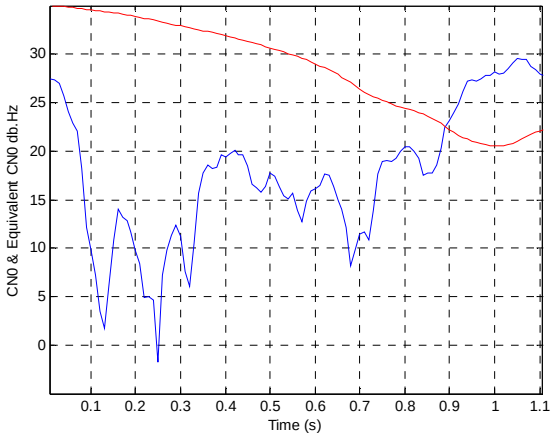

Figure 22: Fades temporal characterisation

As demonstrated above, the depth of the fading cannot be directly linked to C/N0 degradation over the loop integration time. Furthermore the previous result highlights that the advantage to use a narrow loop bandwidth as proposed in the optimised scheme is two fold:

- First the narrow bandwidth enables to decrease the tracking threshold in “static” conditions.
- Second the filtering time span grants an additional in dynamic conditions since it allows to filter most of the short fades due to scintillation.

In order to inject improvement robustness brought by a narrow loop bandwidth the following approach is proposed:

The approach consists in extending the available models to an integration time of one second through the consideration of several independent samples per seconds. Indeed, as mentioned previously the available formula relies on the assumption to have only a single independent sample during the PLL integration time, that is valid for equivalent noise loop bandwidth of 100 Hz or wider. Observation of GISM time series (Figure 21) enables to empirically identify three states within 1-second independent from one another. This means that it can be reasonably assumed to have 3 independent samples within one second.

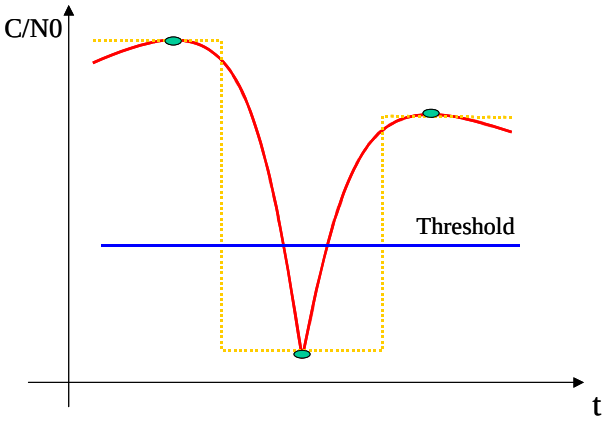

Figure 23: Qualitative description of proposed approach.

Considering this model, the probability not to loose lock is equal to the sum of probability to have one of the four following cases:

- At least one out of the three independent samples above the tracking threshold plus 10*log10(3)=4.7 dB.
- At least two out of the three independent sample above the tracking threshold plus 10*log10(3/2)=1.7 dB
- The three independent samples above the tracking threshold.

Indeed in each case, the equivalent C/N0 over one second cannot be smaller than the tracking threshold. The following table provides some Loss of lock probability over 1 second obtained with this improved model for different S_4 and C/N0.

C/N0 (dB.Hz)	25	30	35
S_4=1	5E-2	2.4E-3	9.1E-5
S_4=0.9	3.3E-2	8.2E-4	1.4E-5
S_4=0.5	3E-4	3.3E-9	<1E-14
S_4=0.3	4E-9	<1E-14	<1E-14

Table 3 : Modified Theoretical Loss Of Lock performance with 18 dB.Hz

C/N0 (dB.Hz)	25	30	35
S_4=1	4.6E-5	1.6E-6	5E-8
S_4=0.9	6.2E-6	9.3E-8	1.4E-9
S_4=0.5	<1E-14	<1E-14	<1E-14
S_4=0.3	<1E-14	<1E-14	<1E-14

Table 4 : Modified Theoretical Loss Of Lock performance with 7 dB.Hz

In order to underline the complexity of the interaction between the tracking threshold and the integration time, the following table provides the loss of lock performance estimated for a loop with a tracking threshold of 12 dB.Hz and an integration time of 200 ms (5 Hz).

Since as demonstrated above, the loop robustness in severe scintillation conditions is a trade off between tracking threshold and integration time, it is not obvious that a loop with 13 dB.Hz tracking threshold is more robust than one with 18 dB.Hz tracking threshold. Indeed the following table computed with a 12 dB.Hz threshold but a single independent sample within the integration time exhibits more degraded results than a 18 dB.Hz threshold with 1 second integration time.

C/N0 (dB.Hz)	25	30	35
S_4=1	6.2E-2	2.0E-2	6.5E-3
S_4=0.9	3.7E-2	9.3E-3	2.3E-3
S_4=0.5	1.43E-4	1.7E-6	1.8E-8
S_4=0.3	2.16E-10	<1E-14	<1E-14

Table 5 : Modified Theoretical Loss Of Lock performance with 13 dB.Hz

Note that in case of 1 Hz loop bandwidth, the fact to consider three independent samples in an integration time of 1 second remains pessimistic since it makes the implicit assumption that the fades stays at its lowest value for 333 ms that is something that has never been observed on the different trials performed with the GISM model. The following figure shows the equivalent of Figure 21 but considering a time duration of 333 ms. It can be seen that although some of the curves start to have a profile more constant during the lap of time considered, this is still not the case for the majority of the deepest fading observed.

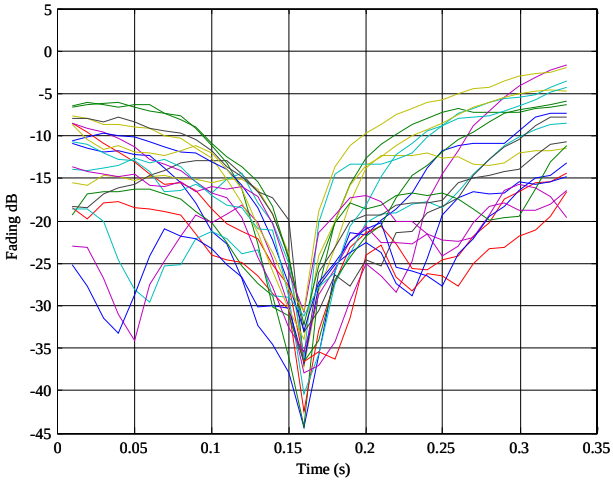

Figure 24: Fades temporal characterisation over 333 milliseconds

It can still be observed a strong difference between the deepest fading observed on 333 ms and the available power integrated in the same period. This difference is measured in between 13 and 32 dB. Actually it decreases in an inverse manner with respect to peak depth, which tends to demonstrate that the deepest fades are also the shortest ones. Based on such observation some more optimisation could still be considered. It show also that the proposed alternative for loss of lock estimation remains to some extent conservative.

CONCLUSIONS

Galileo system is designed in order to provide safety of life service with high continuity and availability performance in severe environment conditions. One of the phenomena that may drive the final performance of the system is the ionosphere scintillation . The first step in order to assess the impact of scintillation on the Galileo performance is to analyse Galileo ground sensor station response to this phenomena. Indeed, scintillation tends to induce deep fadings eventually leading to loss of lock.

Analysis presented in this paper tends to demonstrate that the optimum with respect to the scintillation phenomena as simulated by the GISM model and the Galileo integrity constraint is to select a narrow loop bandwidth of 1 Hertz. Such tuning demonstrated a certain robustness in terms of tracking in severe scintillation conditions. Nevertheless this was not corroborated by the theoretical model used order to extrapolate the continuity performance at system level. Analysis of those model and comparison with the fading dynamic demonstrated that it was not adequate to the Galileo ground receiver context since relying somehow on a wide loop assumption.

An alternative to this model has been proposed in this paper in order to inject the additional robustness brought by a narrow loop bandwidth against the scintillation phenomena. It enables to consider less pessimistic result in the system analysis.

Nevertheless, it should be highlighted that this is not the end of the story regarding the impact of scintillation on Galileo system. Indeed, the receiver is not the only aspect of the system that is impacted. Even if the Galileo receiver can maintain tracking, it shall not be taken for granted that the integrity algorithms are able to process those raw measurements potentially corrupted by high phase noise or cycle slips. Both receiver and algorithm aspects would need to be considered in order to finally present on complete picture regarding the continuity performance of the system. Such analysis are currently on going in the frame of the Critical Design Review of the Galileo Mission ground Segment to be completed by mid 2008.

ACKNOWLEDGEMENTS

This analysis is performed in the frame of ESA contract for Galileo ground segment development. The content of this material reflects the views of the authors, and is not to be considered as an official statement from the Galileo program.

REFERENCES

[01] Felix Butsch, ”Analysis of Potential Ionospheric Common Failure Modes”, EUROCAE WG62 Working Paper - July 2003

[02] Mark Knight, Anthony Finn, “The Effects of Ionospheric Scintillation on GPS”, ION GPS-98, pp 673-685

[03] “Characterization of Ionosphere Scintillation for Galileo” - ESA-APPNG-TN/00255

[04] GISM Technical Manual

[05] “Definition of Ionospheric scintillation scenarios” - GMS internal document

[06] Optimisation of Galileo GRC receivers in ionospheric scintillation conditions, H. Guichon, N. Martin, S. Lannelongue, M.Crisci, ION National technical meeting 2008.